ORIGINAL RESEARCH

Impact of Ischemic and Valvular Heart Disease on Atrial Excitation: A High-Resolution Epicardial Mapping Study

Elisabeth M. J. P. Mouws, MD; Eva A. H. Lanters, MD; Christophe P. Teuwen, MD; Lisette J. M. E. van der Does, MD; Charles Kik, MD; Paul Knops, BSc; Ameeta Yaksh, MD, PhD; Jos A. Bekkers, MD, PhD; Ad J. J. C. Bogers, MD, PhD; Natasja M. S. de Groot, MD, PhD

***Background*—**The influence of underlying heart disease or presence of atrial fibrillation (AF) on atrial excitation during sinus rhythm (SR) is unknown. We investigated atrial activation patterns and total activation times of the entire atrial epicardial surface during SR in patients with ischemic and/or valvular heart disease with or without AF.

***Methods and Results*—**Intraoperative epicardial mapping (N=128/192 electrodes, interelectrode distances: 2 mm) of the right atrium, Bachmann's bundle (BB), left atrioventricular groove, and pulmonary vein area was performed during SR in 253 patients (186 male [74%], age 66±11 years) with ischemic heart disease (N=132, 52%) or ischemic valvular heart disease (N=121, 48%). As expected, SR origin was located at the superior intercaval region of the right atrium in 232 patients (92%). BB activation occurred via 1 wavefront from right-to-left (N=163, 64%), from the central part (N=18, 7%), or via multiple wavefronts (N=72, 28%). Left atrioventricular groove activation occurred via (1) BB: N=108, 43%; (2) pulmonary vein area: N=9, 3%; or (3) BB and pulmonary vein area: N=136, 54%; depending on which route had the shortest interatrial conduction time (P<0.001). Ischemic valvular heart disease patients more often had central BB activation and left atrioventricular groove activation via pulmonary vein area compared with ischemic heart disease patients (N=16 [13%] versus N=2 [2%]; P=0.009 and N=86 [71%] versus N=59 [45%]; P<0.001, respectively). Total activation times were longer in patients with AF (AF: 136±20 [92–186] ms; no AF: 114±17 [74–156] ms; P<0.001), because of prolongation of right atrium (P=0.018) and BB conduction times (P<0.001).

***Conclusions*—**Atrial excitation during SR is affected by underlying heart disease and AF, resulting in alternative routes for BB and left atrioventricular groove activation and prolongation of total activation times. Knowledge of atrial excitation patterns during SR and its electropathological variations, as demonstrated in this study, is essential to further unravel the pathogenesis of AF. **(*J Am Heart Assoc*. 2018;7:e008331. DOI: 10.1161/JAHA.117.008331.)**

Key Words: atrial fibrillation • coronary artery disease • sinus rhythm • valvular regurgitation

Excitation of the atria is determined by membrane properties, tissue structure, and wavefront geometry.[1–3] Knowledge of atrial patterns of activation during sinus rhythm (SR) may enable detection of propagation abnormalities associated with development of atrial tachyarrhythmias such as atrial fibrillation (AF). Prior mapping studies demonstrated that electrical activity originating from the sinus node area, after having spread towards the superior vena cava and the right atrial appendage, propagated from the right atrium (RA) to the left atrium (LA) via Bachmann's bundle (BB), the rim of the fossa ovalis region, or the coronary sinus ostial connections.[4–6] In these mapping studies, patterns of activation were reproducible and showed limited interindividual variation. In vivo activation mapping of the entire RA and LA during SR has only been performed in a limited number of patients with a low spatial resolution. In addition, most mapping studies were performed on the endocardial surface and therefore did not include direct measurements of conduction along BB. At present, it is unknown whether atrial activation patterns, including interatrial conduction, are influenced by underlying heart disease or the presence of AF episodes. As patients with valvular heart disease are more susceptible to develop AF than patients with coronary artery disease, atrial activation patterns may also differ during SR.[7]

The aims of the present study are therefore to investigate in a large cohort of patients with ischemic and/or valvular

From the Departments of Cardiology (E.M.J.P.M., E.A.H.L., C.P.T., L.J.M.E.v.d.D., P.K., A.Y., N.M.S.d.G.), and Cardiothoracic Surgery (E.M.J.P.M., C.K., J.A.B., A.J.J.C.B.), Erasmus Medical Center, Rotterdam, the Netherlands.

An accompanying Figure S1 is available at http://jaha.ahajournals.org/content/7/6/e008331/DC1/embed/inline-supplementary-material-1.pdf

Correspondence to: Natasja M. S. de Groot, MD, PhD, Unit Translational Electrophysiology, Department of Cardiology, Erasmus Medical Center, 's Gravendijkwal 230, 3015CE Rotterdam, the Netherlands. E-mail: nmsdegroot@yahoo.com

Received December 10, 2017; accepted February 9, 2018.

Clinical Perspective

What Is New?

- Our data demonstrate the impact of underlying heart disease, atrial fibrillation episodes, and patient characteristics on sinus rhythm activation patterns.
- In addition, our data show the susceptibility of Bachmann's bundle for damage and its effect on atrial excitation, particularly in patients with valvular heart disease.

What Are the Clinical Implications?

- Our findings provide unique insights in alterations in atrial excitation, which also play a role in the pathogenesis of atrial fibrillation, thereby contributing to novel insights into the development of atrial fibrillation.

heart disease whether atrial patterns of activation and total excitation time of the RA and LA are influenced by patient characteristics and the presence of AF episodes.

Methods

The data, analytic methods, and study materials will not be made available to other researchers for purposes of reproducing the results or replicating the procedure.

Study Population

The study population consisted of 253 successive adult patients undergoing elective open heart coronary artery bypass grafting, aortic or mitral valve surgery, or a combination of valvular and bypass grafting surgery in the Erasmus Medical Center Rotterdam. This study was approved by the institutional medical ethical committee (MEC2010-054/MEC2014-393)[8,9]; written informed consent was obtained from all patients. Preoperative ECG and clinical data were extracted from electronic patient files. Preoperative surface ECGs were screened for the occurrence of interatrial block based on the Bayes criteria.[10]

Mapping Procedure

Epicardial high-resolution mapping was performed before commencement of extracorporeal circulation, as previously described in detail.[11–13] A temporary bipolar epicardial pacemaker wire was stitched to the RA free wall, serving as a temporal reference electrode. The indifferent electrode consisted of a steel wire fixed to subcutaneous tissue of the thoracic cavity.

Epicardial mapping was performed with a 128-electrode array, which was later replaced by a 192-electrode array to shorten the duration of the mapping procedure (electrode diameter 0.65 mm or 0.45 mm, respectively, interelectrode distances 2 mm). Mapping was conducted by shifting the electrode array along predefined areas of the RA, BB, and LA between anatomical borders in a systematic order, covering the entire atrial epicardial surface, in which omission of areas was avoided at the expense of possible small overlap between successive mapping sites, as illustrated in the upper left panel of Figure 1. The RA was mapped in 4 consecutive horizontal lines (RA1-4) from the cavotricuspid isthmus towards the right atrial appendage, perpendicular to the inferior and superior caval vein. Mapping of BB was performed from the border of the left atrial appendage towards the superior cavo-atrial junction. The pulmonary vein area (PVA) was mapped from the sinus transversus along the borders of the right and left pulmonary veins down towards the atrioventricular groove. The left atrioventricular groove (LAVG) was mapped from the lower border of the left inferior pulmonary vein (LA1) towards the left atrial appendage (LA2).

Five seconds of SR were recorded at every mapping site, including a surface ECG lead, a calibration signal of 2 mV and 1000 ms, a bipolar reference electrogram, and all unipolar epicardial electrograms.[11]. Recordings were sampled with a rate of 1 kHz, amplified (gain 1000), filtered (bandwidth 0.5–400 Hz), analog-to-digital converted (16-bits), and stored on a hard disk.[11]

Activation Mapping of the Atrial Epicardium

The upper left panel of Figure 1 shows all mapping locations, including RA1-4, BB, LA, and right and left pulmonary veins, on a schematic view of the atria.

Examples of activation maps obtained from each of these sites are displayed in the upper right panel of Figure 1. Local activation maps during 5 s of SR were constructed by annotating the steepest negative slope of atrial potentials recorded at every electrode. Atrial extrasystolic beats were excluded from analysis.[14–16] In order to reconstruct activation patterns of the entire epicardial surface, the time interval between the local activation time of the reference electrode (defined as zero point) and every electrode was calculated and depicted in color-code, as demonstrated in the total activation map in the lower right panel of Figure 1. Figure S1 provides a more extensive view of annotation of electrograms and construction of activation maps, enabling the display of the total activation map.

In this example, the epicardial surface of RA is first excited by a broad wavefront originating from the superior intercaval region. This wavefront then spreads across the RA and BB, towards the LA. In the LA, another wavefront

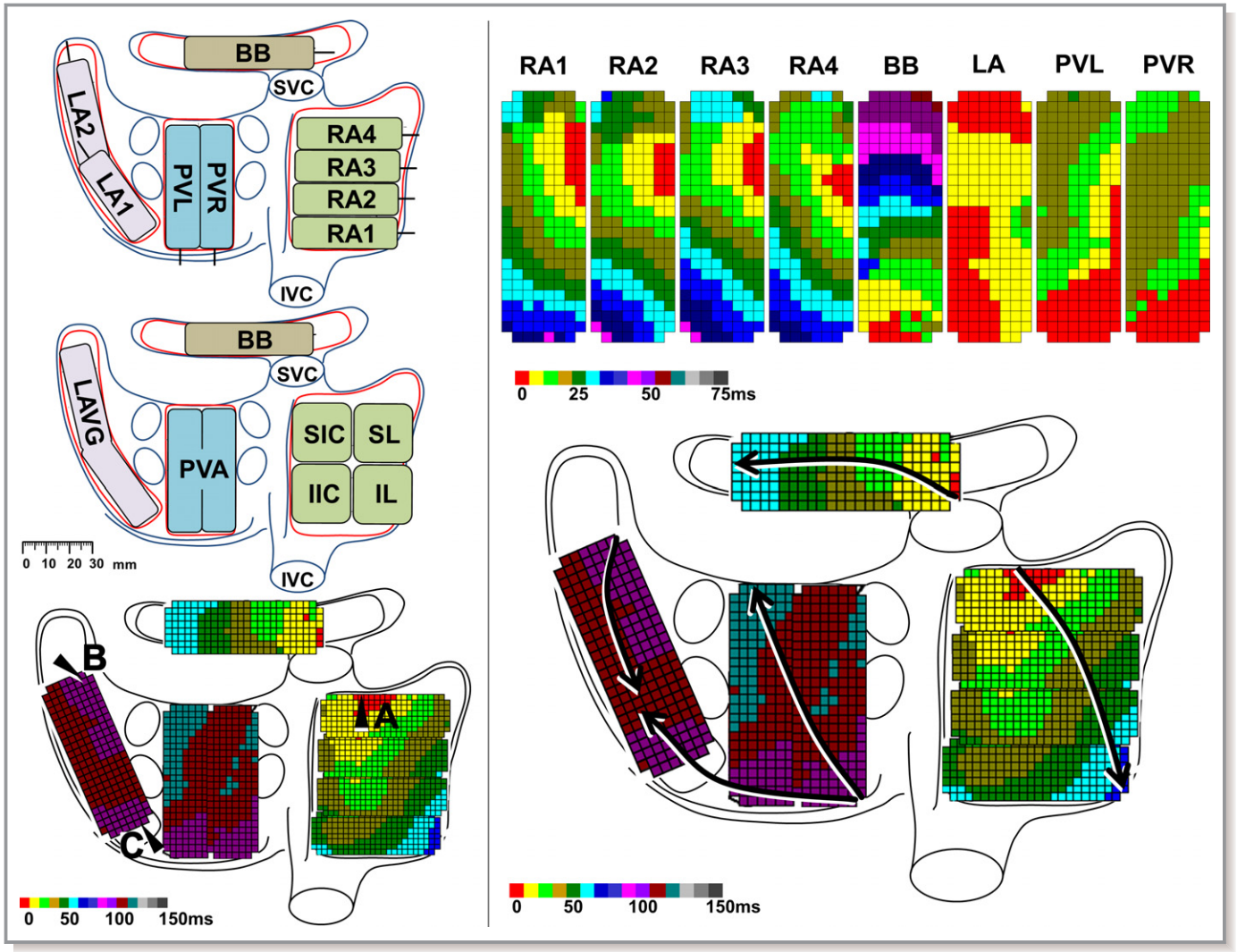

Figure 1. Activation mapping of the right and left atrium. *Left panel:* Posterior view of the atria with epicardial mapping scheme (192 electrodes) *(upper)*, classification of the anatomical regions *(middle)*, and landmarks for calculation of duration of wavefront propagation from the origin of sinus rhythm (A) to the LAVG via BB (B) and via PVA (C). *Upper right panel:* Color-coded activation maps per mapping site; electrodes activated within the first 5 ms are colored red. *Lower right panel:* Total activation map constructed relative to local activation times of the reference electrode, which was defined as 0 ms. Arrows indicate main trajectories of SR waves at the different atrial regions. BB indicates Bachmann's bundle; IIC, inferior intercaval; IL, inferolateral; IVC, inferior vena cava; LA, left atrium; LAVG, left atrioventricular groove; PVA, pulmonary vein area; PVL, pulmonary veins left; PVR, pulmonary veins right; RA, right atrium; SIC, superior intercaval; SL, superolateral; SR, sinus rhythm; SVC, superior vena cava.

emerges in the coronary sinus region and propagates towards the left upper pulmonary vein. The LAVG is thus activated by 2 wavefronts, originating from both BB and PVA, merging in the middle of the LAVG.

Total activation times were calculated as the time interval (ms) between the earliest and latest activated electrode. As visualized in the lower left panel of Figure 1, the duration of propagation was calculated for wavefronts propagating from the origin of SR across BB towards the LAVG (Figure 1, point A to point B) and for wavefronts propagating from the SR origin through the limbus of the fossa ovalis or the coronary sinus ostium across the PVA towards the LAVG (Figure 1, point A to point C). The latter conduction route will be referred to as conduction via PVA.

Classification of Patterns of Activation

Patterns of activation and propagation direction were examined in all SR maps. The origin of RA activation was assigned to 1 of the 4 regions demonstrated in the lower left panel of Figure 1, including the superior intercaval, inferior intercaval, superolateral and inferolateral region.

Entry sites of SR wavefronts in BB were classified as right atrial, central, left atrial, or multiple entry sites. A right atrial

entry site was defined as a wavefront first entering the mapping array from the right side of BB, propagating towards the left side of BB, whereas in case of a left atrial entry site the initial activation was observed at the tip of the electrode positioned at the border of the left atrial appendage, spreading towards the right side of BB. A wavefront emerging in the middle of the mapping array propagating to either the right and/or left side was labeled as a central entry site. Excitation of the LAVG was described as activation via BB only, the PVA only, or a combination of both.

Statistical Analysis

Normally distributed data are described by mean±SD (minimum–maximum) and analyzed with a Student *t* test or a 1-way ANOVA. Skewed data are described by median (minimum–maximum) and analyzed with Kruskal–Wallis test or a Mann–Whitney *U* test. Categorical data are expressed as numbers and percentages and analyzed with χ^2 or Fisher exact test when appropriate. Multiple linear regression analysis was performed to identify independent predictors for prolonged total activation times. A *P* value <0.05 was considered statistically significant. All statistical analyses were performed with IBM SPSS statistics for Windows, version 24 (IBM Corp, Armonk, NY).

Results

Study Population

Characteristics of the study population (N=253, 186 male [74%], age 66±11 years) are summarized in Table 1. Patients had either ischemic heart disease (IHD) (N=132, 52%), valvular heart disease (VHD) (N=68, 27%), or a combination of valvular and ischemic heart disease (I/VHD) (N=53, 21%). VHD (N=121) was categorized by the predominant valvular lesion and consisted of aortic valve stenosis (N=68, 27%), aortic valve insufficiency (N=9, 4%), or mitral valve insufficiency (N=44, 17%).

A minority of patients (N=43, 17%) had a history of AF, of whom 13 presented in AF and underwent SR mapping after electrocardioversion.

AF was most prevalent in patients with mitral valve disease (N=16, 36%) compared with patients with aortic valve disease (N=14, 18%) or only ischemic heart disease (N=13, 10%) (*P*<0.001). Also, AF was more prevalent in patients with LA dilation (N=16, 30%) compared with patients without LA dilation (N=27, 14%) (*P*=0.004). Most patients had a normal left ventricular function (N=188, 74%) and the majority used class II (N=165, 65%) antiarrhythmic drugs. Patients were mapped with either a 128-polar (N=141, 56%) or a 192-polar electrode array (N=112, 44%). Mean cycle length was 857±175 (473–1458) ms.

Table 1. Patient Characteristics

	Total
Number of patients	253
Age, y	66±11 (21–84)
Male	186 (74)
BSA	2.0±0.2 (1.5–2.8)
Underlying heart disease	N (%)
IHD	132 (52)
VHD	68 (27)
I/VHD	53 (21)
Valvular heart disease	121 (48)
Aortic valve stenosis	68 (27)
Mild	2 (1)
Moderate	14 (5)
Severe	52 (21)
Aortic valve insufficiency	9 (4)
Mild	1 (1)
Moderate	5 (2)
Severe	3 (1)
Mitral valve insufficiency	44 (17)
Moderate	14 (5)
Severe	30 (12)
Left atrial dilation	53 (21)
History of AF	43 (17)
Paroxysmal	33 (13)
Persistent	9 (4)
Longstanding persistent	1 (1)
Left ventricular function	
Normal	188 (74)
Mild dysfunction	46 (18)
Moderate dysfunction	17 (7)
Severe dysfunction	2 (1)
Antiarrhythmic drugs	175 (69)
Class I	1 (1)
Class II	165 (65)
Class III	8 (3)
Class IV	2 (1)

AF indicates atrial fibrillation; BSA, body surface area; I/VHD, ischemic and valvular heart disease; IHD, ischemic heart disease; VHD, valvular heart disease.

Compared with IHD patients, (i)VHD patients more often had LA dilation (*P*=0.007) and AF (*P*=0.001), which was more often (longstanding) persistent (*P*=0.007). IHD patients more often used β-blockers (*P*<0.001).

For all performed analyses as described in the Results section, there were no differences between patients with VHD

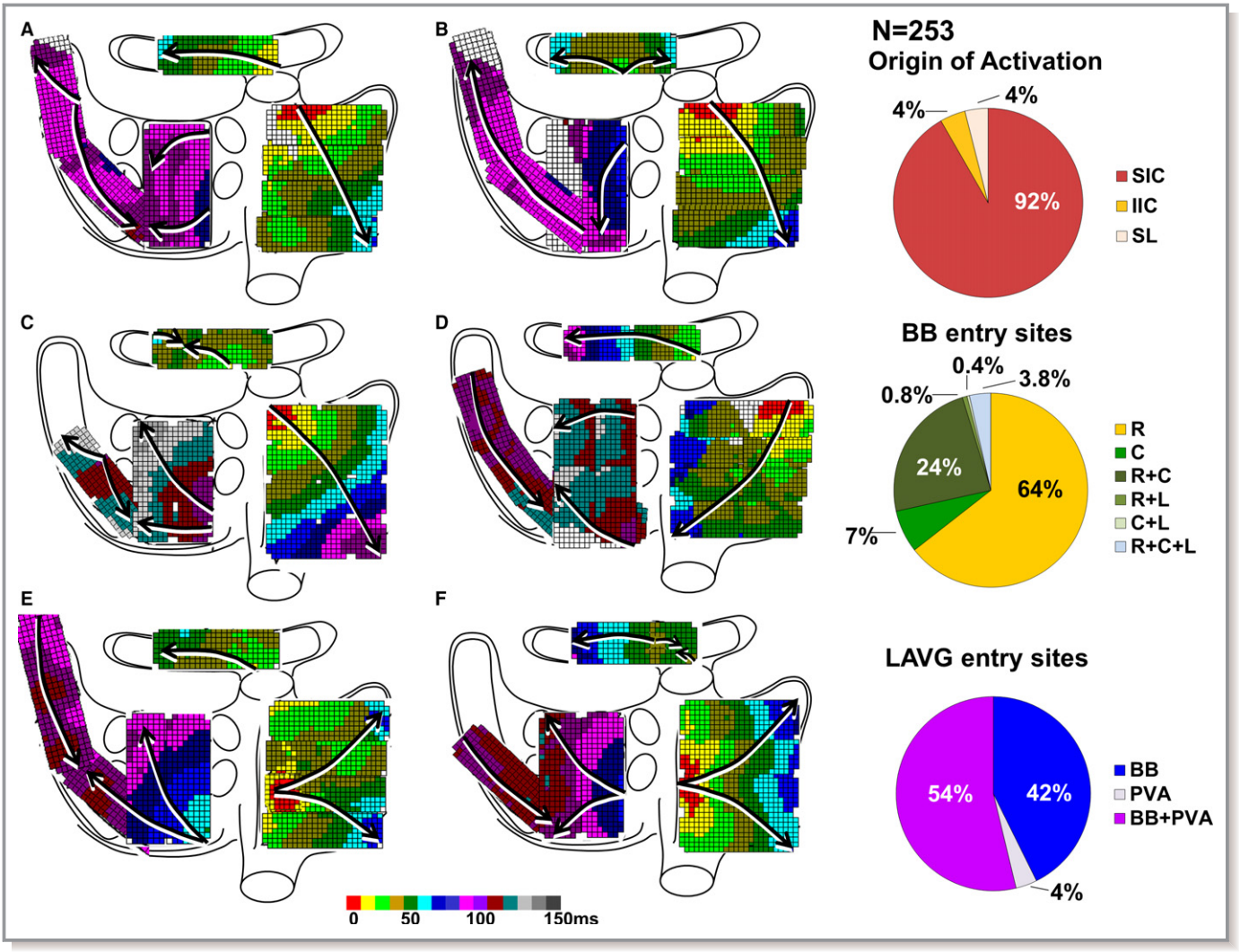

Figure 2. Atrial patterns of activation. *Left panel:* Examples of excitation of the atrial epicardial surface during SR. Arrows indicate main trajectories of SR waves at the different atrial regions; *see text for detailed explanation*. *Right panel:* Relative incidences of different locations of the origin of activation, entry sites at BB and the LAVG. BB indicates Bachmann's bundle; C, central; IIC, inferior intercaval; L, left; LAVG, left atrioventricular groove; PVA, pulmonary vein area; R, right; SIC, superior intercaval; SL, superolateral; SR, sinus rhythm.

or I/VHD; therefore, these 2 patient groups were combined and referred to as (i)VHD in order to assess the influence of VHD on activation times and patterns when comparing these patients with patients with isolated IHD. Also, differences between IHD and (i)VHD patients as described in the Results section could not be explained by the abovementioned differences in clinical characteristics.

Origin of Atrial Activation

Figure 2 shows 6 typical examples of different patterns of activation observed in our study population. The origin of atrial activation was located in the superior intercaval region in 232 patients (92%; Figure 2A through 2C). In the remaining patients, earliest activation was identified in the superolateral region (N=10, 4%; Figure 2D) or in the inferior intercaval region (N=11, 4%; Figure 2E and 2F). As expected, the location of the origin of atrial activation did not differ between patients with or without AF (P=0.344) and between patients with IHD or (i)VHD (P=0.181). In addition, cycle length did not differ between the various locations of the SR origin (superior intercaval: 858±178 [473–1458] ms; superolateral: 832±162 [646–1081] ms; inferior intercaval: 861±114 [666–1046] ms, P=0.894).

Excitation of BB

Conduction along BB occurred mainly by a single wavefront, propagating from the right to the left side (N=163, 64%), as shown in Figure 2A, 2D, and 2E. Figure 2B demonstrates central activation of BB spreading towards both the right and left side; this pattern of activation occurred in 18 patients (7%).

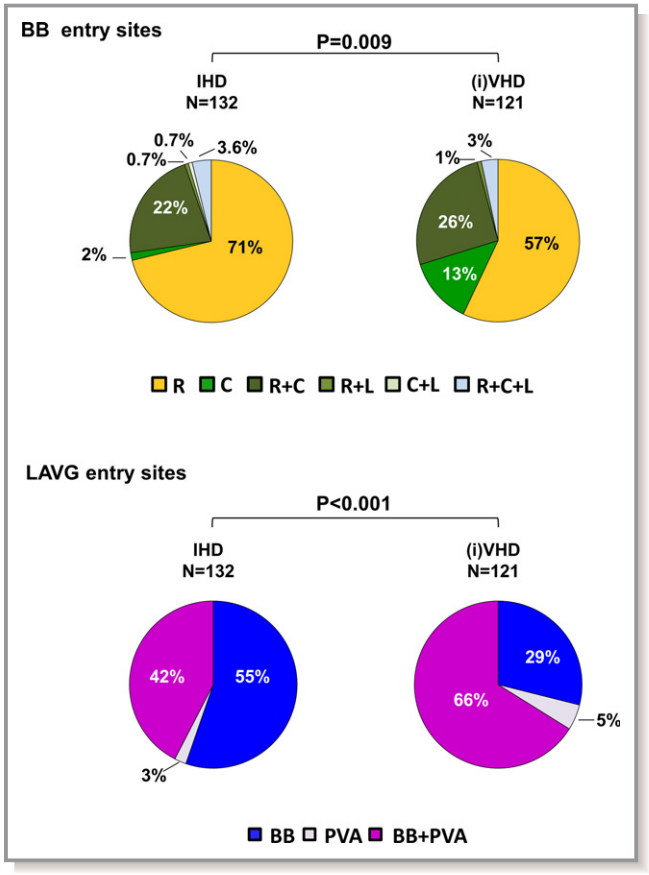

Figure 3. Activation of Bachmann's bundle and the left atrioventricular groove. Differences in incidences of entry sites of wavefronts at BB and LAVG between patients with IHD and (i)VHD. (i)VHD indicates (ischemic and) valvular heart disease; BB, Bachmann's bundle; C, central; IHD, ischemic heart disease; L, left; LAVG, left atrioventricular groove; PVA, pulmonary vein area; R, right.

Activation of BB by multiple wavefronts originating from different entry sites was observed in 72 patients (29%). In 60 of these patients (83%), BB was activated by 2 separate wavefronts entering from the right side and from the central part of BB (Figure 2F). A combination of 2 wavefronts entering from the right and left side occurred in 2 patients (3%) (Figure 2C) and 1 patient (1%) showed activation of BB via the central part and the left side. In 9 patients (13%), BB was activated by 3 wavefronts entering from the right, left, and central part of BB.

BB activation patterns and the number of entry sites did not differ between patients without and with a history of AF (P=0.570 and P=0.388, respectively).

As illustrated in the upper panel of Figure 3, patterns of wavefront propagation along BB differed between IHD and (i)VHD (P=0.009). A wavefront entering in the central part of BB was observed most frequently in patients with (i)VHD (N=16, 13%) compared with IHD patients (N=2, 2%). BB activation patterns did not differ between patients with aortic or mitral VHD (P=0.409) The number of entry sites in BB was similar between IHD and (i)VHD (P=0.557).

Excitation of the LAVG

Typical examples of activation patterns of the LAVG are shown in Figure 2. As illustrated in Figure 2A through 2E, most patients (N=136, 54%) showed activation of the LAVG by 2 wavefronts originating from both BB and the PVA, indicating propagation of conduction through the fossa ovalis and the coronary sinus ostium. A single wavefront activating the LAVG via only BB (Figure 2F) or PVA (Figure 2B) occurred in 108 (42%) and 9 (4%) patients, respectively. Location of the origin of SR did not influence the preferential use of either BB or PVA for interatrial propagation (P=0.871).

Preferential interatrial routes for LAVG excitation were similar between patients without and with AF (P=0.224); LAVG activation via: (1) a combination of BB and PVA (without AF: N=109, 52%; with AF: N=27, 63%); (2) BB only (without AF: N=92, 44%; with AF: N=16, 37%); or (3) PVA only (without AF: N=9, 4%; with AF: N=0).

However, use of interatrial routes differed between patients with IHD and (i)VHD (P<0.001). As displayed in the lower panel of Figure 3, activation via BB only was most frequently observed in IHD patients (N=73, 55%). In patients with (i)VHD, LAVG activation via BB only was observed in only 29% of patients (N=35), whereas propagation through the interatrial septum via the fossa ovalis or the coronary sinus across the PVA occurred in 86 patients (71%), of whom 6 patients (5%) showed LAVG activation via the PVA only. Type of VHD did not influence the use of different conduction routes (P=0.760).

Examination of surface ECGs showed a mean P-wave duration of 98±16 ms; P-wave duration was ≥120 ms in 58 patients (23%). However, complete interatrial conduction block according to the Bayes criteria in the inferior leads could not be confirmed in these patients. The incidence of partial interatrial block, defined by only a prolongation of P-wave duration ≥120 ms on the surface ECG, was similar for patients without and with AF (N=51 [24%] versus N=7 [16%], respectively, P=0.255), as well as for patients without and with LA dilation (N=45 [23%] versus N=13 [25%], respectively, P=0.755). Also, preferential routes of conduction towards the LAVG did not differ between those with a P-wave duration <120 ms and ≥120 ms.

Conduction Time Towards the LAVG

As depicted in Figure 1, conduction times towards the LAVG via BB or via PVA were assessed by calculation of the time interval between point A and B and between point A and C, respectively. Time required for wavefronts to propagate from the SR origin to

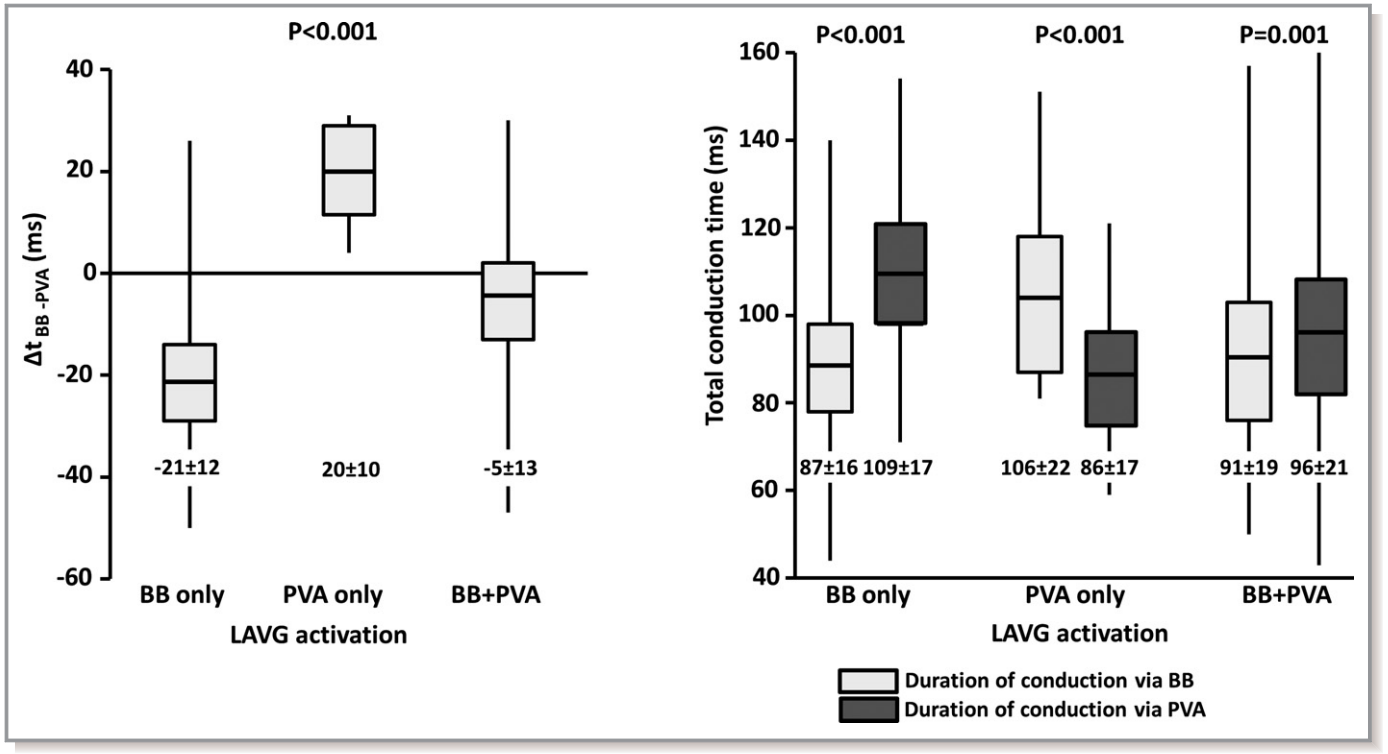

Figure 4. Conduction times towards the left atrioventricular groove. Time differences *(left panel)* and total conduction times *(right panel)* between BB and PVA conduction routes towards LAVG in patients with LAVG activation via BB only, PVA only, or BB and PVA. BB indicates Bachmann's bundle; LAVG, left atrioventricular groove; PVA, pulmonary vein area.

the LAVG via BB was 90±18 (44–157) ms, while propagation to the LAVG via PVA was 101±20 (43–160) ms (P<0.001).

Figure 4 illustrates the differences in conduction times *towards* the LAVG, which were larger in those with 1 predominant route (BB or PVA), compared with those with a route via both BB and PVA (P<0.001). If LAVG was activated via both BB and PVA (N=136), total conduction time along BB was only 5±13 (−47 to +30) ms shorter than via PVA. However, if LAVG was activated only via PVA (N=9), total conduction time via PVA was 20±10 (+4 to +31) ms shorter than via BB (lower panels of Figure 4). Likewise, if LAVG was activated only via BB (N=108), total conduction time via BB was 21±12 (−50 to +26) ms shorter than via PVA.

Duration of Right and Left Atrial Excitation

Total activation time of the entire atrial epicardial surface was 118±19 (74–186) ms. The upper panel of Figure 5 shows differences in total activation times for patients without or with AF, various underlying heart diseases, and without or with LA dilation. Similar data for the different atrial regions are depicted in Table 2.

In patients with a history of AF, total activation times were longer than in patients without a history of AF; mean durations are, respectively, 136±20 (92–186) and 114±17 (74–156) ms (P<0.001). This difference was mainly the result of a significantly longer total activation time of the RA and BB in patients with AF (RA: 73±13 [42–98] ms versus 67±14 [32–142] ms, P=0.018; BB: 106±20 [68–157] ms versus 87±16 [44–151] ms, P<0.001), as demonstrated in the lower panel of Figure 5 and in Table 2. Total activation times of the LA were similar (without AF: 46±15 [6–111] ms; with AF: 48±17 [8–92] ms, P=0.376).

Patients with IHD or (i)VHD had similar total activation times with mean durations of, respectively, 117±17 (74–156) ms and 119±21 (77–186) ms (P=0.318). When analyzing the difference between IHD, AVD, or MVD patients separately, similar total activation times were observed for AVD and IHD patients (total activation time: 116±20 versus 117±17 ms, respectively, P=0.770), whereas MVD patients had significantly longer total activation times than IHD patients (125±23 versus 117±17 ms, respectively, P=0.015). Subsequently, dividing the entire cohort into patients without and with MVD showed longer total activation times in MVD patients compared with patients without MVD (125±23 versus 117±18 ms, respectively, P=0.009, Figure 5). Although no specific site of prolongation of conduction was found, BB showed a trend towards prolongation of conduction in these patients (P=0.096) (Table 2).

As depicted in Table 2, longer total activation times showed a strong association with LA dilation (P<0.001), yet remarkably, this was only because of prolongation of

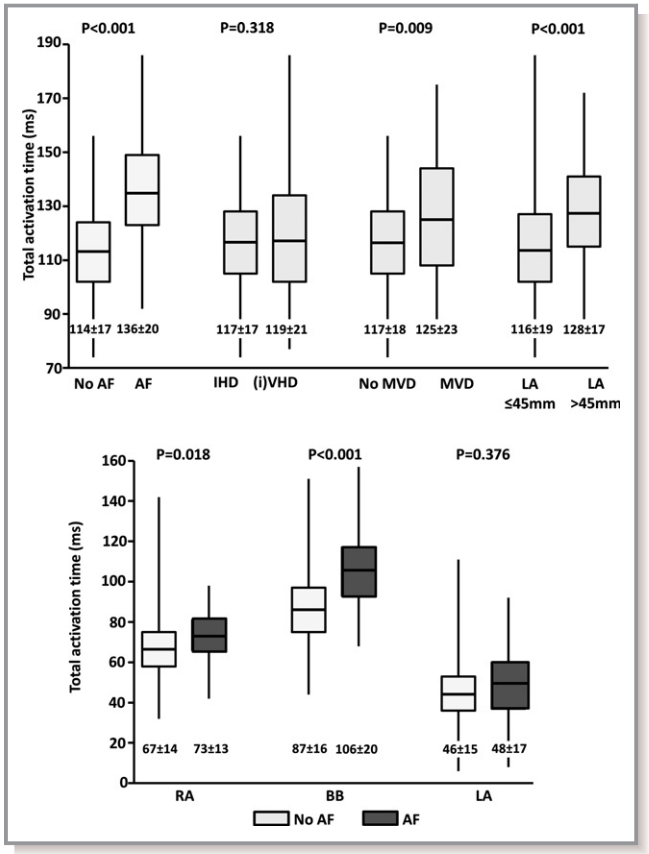

Figure 5. Differences in total activation times. *Upper panel:* Differences in total activation time of the entire atrial surface between patients without and with AF, various underlying heart diseases and without or with LA dilation. *Lower panel:* Differences in total activation time of RA, BB and LA separately between patients without and with AF. (i)VHD indicates (ischemic and) valvular heart disease; AF, atrial fibrillation; BB, Bachmann's bundle; IHD, ischemic heart disease; LA, left atrium; MVD, mitral valve disease; RA, right atrium.

conduction on BB ($P<0.001$), rather than on LA ($P=0.717$). This is mainly the result of the fact that slow conduction on BB was largely compensated by LAVG activation via the PVA route so that LA activation times are not prolonged. As AF, MVD, and LA dilation are closely intertwined, a multivariate analysis was performed in which older age also was taken into account. History of AF (B 18.58 [95% CI, 12.8–24.4], $P<0.001$), LA dilation (B 8.27 [95% CI, 2.8–13.7], $P=0.003$), and older age (B 0.28 [95% CI, 0.08–0.48], $P=0.006$) were independent predictors for prolonged total activation times, whereas MVD (B 0.48 [95% CI, −5.4 to 6.4] $P=0.872$) was not.

Discussion

Key Findings

Intraoperative, high-resolution epicardial mapping of the entire atrial surface during SR demonstrated prolonged excitation of the atria in patients with a history of AF, which was mainly caused by longer total activation times of the RA and BB. Patients with MVD and with LA dilation had the highest prevalence of AF. Remarkably, LA dilation was associated with longer conduction times of BB and not of LA.

In patients with (i)VHD, who most likely have the highest degree of structural remodeling, central BB excitation and interatrial conduction via both BB and PVA towards the LAVG was more prevalent. The predominance of different routes of interatrial conduction depended on conduction time towards the LAVG.

Table 2. Activation Times for Various Underlying Heart Diseases

Activation Times (ms)	No AF	AF	*P* Value
TAT	114±17	136±20	<0.001
BB	87±16	106±20	<0.001
RA	67±14	73±13	0.018
LA	46±15	48±17	0.376
	IHD	(i)VHD	
TAT	117±17	119±21	0.318
BB	88±17	91±19	0.181
RA	69±15	67±13	0.395
LA	47±15	46±15	0.391
	No MVD	MVD	
TAT	117±18	125±23	0.009
BB	89±17	94±22	0.096
RA	68±15	67±12	0.627
LA	46±15	47±17	0.790
	No LA Dilation	LA Dilation	
TAT	116±19	128±17	<0.001
BB	88±17	98±18	<0.001
RA	68±14	69±13	0.741
LA	47±15	46±15	0.717

(i)VHD indicates (ischemic and) valvular heart disease; AF, atrial fibrillation; BB, Bachmann's bundle; IHD, ischemic heart disease; LA, left atrium; MVD, mitral valve disease; RA, right atrium; TAT, total activation time.

Location of the Sinus Node

In coherence with previous studies, we observed a certain variation in the location of the origin of activation along the intercaval line and the superior RA wall.[6,17,18] However, we could not confirm a relation between mean SR cycle length and the various locations of SR origins. Previous studies demonstrated that there is a certain degree of interindividual variety in the location of the sinus node area. Also within a patient, the leading pacemaker site within the sinus node can shift in position, depending on autonomic changes.[17,18]

Boineau et al previously reported a correlation between the spatial position of the sinus origin and the SR cycle length.[19] Faster heart rates were initiated from origins located more superiorly along the sulcus terminalis, whereas slower heart rates were initiated from origins located more inferiorly.[19] Optical mapping studies by Fedorov et al showed delayed sinus node activation followed by fast atrial activation via sinoatrial exit pathways.[20] They found a conduction delay of 82 ms between earliest sinus node excitation and earliest excitation of the atrial myocardium.[20] Though the site of first sinus node excitation remained stable, earliest excitation of the atrial myocardium via the sinoatrial exit pathways could shift inferiorly when SR cycle length prolonged.[20]

Interatrial Conduction

There was a large interindividual variation in activation of BB in our study population. Prior studies have demonstrated muscular connections between BB and the interatrial septum, which can excite the center of BB.[5,21–23] These muscular connections enable wavefronts to conduct via interatrial pathways such as the limbus of the fossa ovalis, the coronary sinus, and interatrial bundles both superior and inferior along BB.[5,23] SR wavefronts may propagate upwards in the interatrial septum and activate the central area of BB. Teuwen et al indeed observed in 185 patients with IHD that lines of conduction block at BB may delay right-to-left excitation, thereby favoring conduction via other interatrial routes, such as the interatrial septum.[23] Conduction via 1 wavefront entering in the central part of BB was reported in 4% of their population and combinations of entry sites involving the central part of BB in 29% of IHD patients.[23] We found similar incidences in our cohort, although there were differences between underlying heart diseases with a far higher incidence of central entry sites in patients with (i)VHD. The overall preferential route of interatrial conduction in our study population was BB, with a right-to-left conduction pattern via a single wavefront in most patients. Also, interatrial conduction via PVA or a combination of BB and PVA was more likely to occur in patients with (i)VHD.

Activation of the LAVG via a wavefront originating at the anterosuperior side and propagating towards the posterior side of the LAVG is in coherence with the exit point of the outer left BB, whereas activation via the posteroseptal wall can be interpreted as wavefronts propagating via the limbus of the fossa ovalis or the coronary sinus ostium.

The predominance of these alternative routes of conduction may be the result of damage to the thick and thin septa surrounding BB myocytes.[24] It has been suggested that increased atrial stretch delays conduction along BB.[24] We hypothesize that this layer is more likely to be damaged first by chronic atrial stretch, which is more pronounced in VHD patients. Damage to this layer may thereby slow BB conduction and give rise to the predominance of activation patterns via alternative routes of interatrial conduction.

This hypothesis was further supported by the observation that in patients with conduction via only PVA, conduction via BB is considerably slower—up to 31 ms—than via PVA.

Particularly patients with AF, LA dilation, or mitral valve disease showed longer total excitation times of the atria, which was all mostly influenced by conduction times along BB. Although MVD, LA dilation, and AF are closely intertwined, our findings suggest that atrial activation times are particularly affected at BB and RA by remodeling because of the presence of AF, which might be secondarily enforced by atrial stretch as a result of MVD.

Interatrial block based on a biphasic *P*-wave morphology in the inferior leads in those with a *P*-wave duration $\geq$120 ms, however, could not be confirmed, nor did preferential routes of conduction towards the LAVG differ between those with a *P*-wave duration $<$120 ms and $\geq$120 ms.

Limitations

Most patients with AF in our study had paroxysmal AF instead of (longstanding) persistent AF. Electrical and structural remodeling in these patients is expected to be less, therefore differences between patients without and with AF in our study might be underestimated.

Whether general anesthesia and intraoperative drugs influence conduction is yet to be investigated; however, a standard anesthetic protocol was used for all patients and SR was confirmed during all mapping procedures. Thus, possible effects of anesthesia would be equally dispersed among the patient population. In addition, high-resolution mapping of the interatrial septum was not performed with our closed beating heart approach.

Conclusions

High-resolution mapping of the atrial epicardial surface during SR in a large cohort of IHD and/or VHD patients demonstrated a considerable interindividual variation in excitation of the atria. RA and LA excitation are affected by underlying heart disease and presence of AF.

BB appears most susceptible to damage caused by MVD, LA dilation, and AF, causing local conduction delay. Central BB excitation and interatrial conduction via both BB and PVA towards the LAVG was more prevalent in patients with (i)VHD, likely resulting from a more severe degree of structural remodeling causing intra-atrial conduction delay. Knowledge about atrial excitation patterns during SR and its electropathological variations, as demonstrated in this study, is essential to further unravel the pathogenesis of AF.

Sources of Funding

Dr Groot is supported by grants from the Erasmus Medical Center fellowship, Dutch Heart Foundation (2012T0046), LSH-Impulse grant 40-43100-98-008, CVON AFFIP (grant no. 914728), and VIDI grant (no. 91717339).

Disclosures

None.

References

1. Fast VG, Kléber AG. Role of wavefront curvature in propagation of cardiac impulse. *Cardiovasc Res*. 1997;33:258–271.
2. Spach MS, Kootsey JM. The nature of electrical propagation in cardiac muscle. *Am J Physiol*. 1983;244:H3–H22.
3. de Bakker JMT, van Rijen HMV. Continuous and discontinuous propagation in heart muscle. *J Cardiovasc Electrophysiol*. 2006;17:567–573.
4. Lemery R, Birnie D, Tang ASL, Green M, Gollob M, Hendry M, Lau E. Normal atrial activation and voltage during sinus rhythm in the human heart: an endocardial and epicardial mapping study in patients with a history of atrial fibrillation. *J Cardiovasc Electrophysiol*. 2007;18:402–408.
5. Tapanainen JM, Jurkko R, Holmqvist F, Husser D, Kongstad O, Mäkijärvi M, Toivonen L, Platonov PG. Interatrial right-to-left conduction in patients with paroxysmal atrial fibrillation. *J Interv Card Electrophysiol*. 2009;25:117–122.
6. Sakamoto S, Yamauchi S, Yamashita H, Imura H, Maruyama Y, Ogasawara H, Hatori N, Shimizu K. Intraoperative mapping of the right atrial free wall during sinus rhythm: variety of activation patterns and incidence of postoperative atrial fibrillation. *Eur J Cardiothorac Surg*. 2006;30:132–139.
7. Psaty BM, Manolio TA, Kuller LH, Kronmal RA, Cushman M, Fried LP, White R, Furberg CD, Rautaharju PM. Incidence of and risk factors for atrial fibrillation in older adults. *Circulation*. 1997;96:2455–2461.
8. van der Does LJME, Yaksh A, Kik C, Knops P, Lanters EAH, Teuwen CP, Oei FBS, van de Woestijne PC, Bekkers JA, Bogers AJJC, Allessie MA, de Groot NMS. QUest for the Arrhythmogenic Substrate of Atrial fibRillation in Patients Undergoing Cardiac Surgery (QUASAR Study): rationale and design. *J Cardiovasc Transl Res*. 2016;9:194–201.
9. Lanters EAH, van Marion DMS, Kik C, Steen H, Bogers AJJC, Allessie MA, Brundel BJJM, de Groot NMS. HALT & REVERSE: Hsf1 activators lower cardiomyocyte damage; towards a novel approach to REVERSE atrial fibrillation. *J Transl Med*. 2015;13:347.
10. Conde D, Seoane L, Gysel M, Mitrione S, Bayés De Luna A, Baranchuk A. Bayés' syndrome: the association between interatrial block and supraventricular arrhythmias. *Expert Rev Cardiovasc Ther*. 2015;13:541–550.
11. Yaksh A, van der Does LJ, Kik C, Knops P, Oei FB, van de Woestijne PC, Bekkers JA, Bogers AJ, Allessie MA, de Groot NM. A novel intra-operative, high-resolution atrial mapping approach. *J Interv Card Electrophysiol*. 2015;44:221–225.
12. Kik C, Mouws EMJP, Bogers AJJC, de Groot NM. Intra-operative mapping of the atria: the first step towards individualization of atrial fibrillation therapy? *Expert Rev Cardiovasc Ther*. 2017;15:537–545.
13. Mouws EMJP, Lanters EAH, Teuwen CP, van der Does LJME, Kik C, Knops P, Bekkers JA, Bogers AJJC, de Groot NMS. Epicardial breakthrough waves during sinus rhythm. *Circ Arrhythm Electrophysiol*. 2017;10:e005145.
14. de Groot N, van der Does L, Yaksh A, Lanters E, Teuwen C, Knops P, van de Woestijne P, Bekkers J, Kik C, Bogers A, Allessie M. Direct proof of endo-epicardial asynchrony of the atrial wall during atrial fibrillation in humans. *Circ Arrhythm Electrophysiol*. 2016;9:e003648.
15. de Groot N, Houben R, Smeets J, Boersma E, Schotten U, Schalij M, Crijns H, Allessie M. Electropathological substrate of longstanding persistent atrial fibrillation in patients with structural heart disease: epicardial breakthrough. *Circulation*. 2010;122:1674–1683.
16. Allessie MA, De Groot NMS, Houben RPM, Schotten U, Boersma E, Smeets JL, Crijns HJ. Electropathological substrate of long-standing persistent atrial fibrillation in patients with structural heart disease: longitudinal dissociation. *Circ Arrhythm Electrophysiol*. 2010;3:606–615.
17. Boineau JP, Canavan TE, Schuessler RB, Cain ME, Corr PB, Cox JL. Demonstration of a widely distributed atrial pacemaker complex in the human heart. *Circulation*. 1988;77:1221–1237.
18. Stiles MK, Brooks AG, Roberts-Thomson KC, Kuklik P, John B, Young GD, Kalman JM, Sanders P. High-density mapping of the sinus node in humans: role of preferential pathways and the effect of remodeling. *J Cardiovasc Electrophysiol*. 2010;21:532–539.
19. Boineau J, Schuessler R, Roeske W, Autry L, Miller C, Wylds A. Quantitative relation between sites of atrial impulse origin and cycle length. *Am J Physiol*. 1983;245:H781–H789.
20. Fedorov VV, Glukhov AV, Chang R, Kostecki G, Aferol H, Hucker WJ, Wuskell JP, Loew LM, Schuessler RB, Moazami N, Efimov IR. Optical mapping of the isolated coronary-perfused human sinus node. *J Am Coll Cardiol*. 2010;56:1386–1394.
21. Ho SY, Sanchez-Quintana D, Cabrera JA, Anderson RH. Anatomy of the left atrium: implications for radiofrequency ablation of atrial fibrillation. *J Cardiovasc Electrophysiol*. 1999;10:1525–1533.
22. Platonov PG, Mitrofanova L, Ivanov V, Ho SY. Substrates for intra-atrial and interatrial conduction in the atrial septum: anatomical study on 84 human hearts. *Heart Rhythm*. 2008;5:1189–1195.
23. Teuwen CP, Yaksh A, Lanters EAH, Kik C, van der Does LJME, Knops P, Taverne YJHJ, van de Woestijne PC, Oei FBS, Bekkers JA, Bogers AJJC, Allessie MA, de Groot NMS. Relevance of conduction disorders in Bachmann's Bundle during sinus rhythm in humans. *Circ Arrhythm Electrophysiol*. 2016;9:e003972.
24. van Campenhout MJH, Yaksh A, Kik C, de Jaegere PP, Ho SY, Allessie MA, de Groot NMS. Bachmann's Bundle: a key player in the development of atrial fibrillation? *Circ Arrhythm Electrophysiol*. 2013;6:1041–1046.

SUPPLEMENTAL MATERIAL

Figure S1. Construction of total SR map.

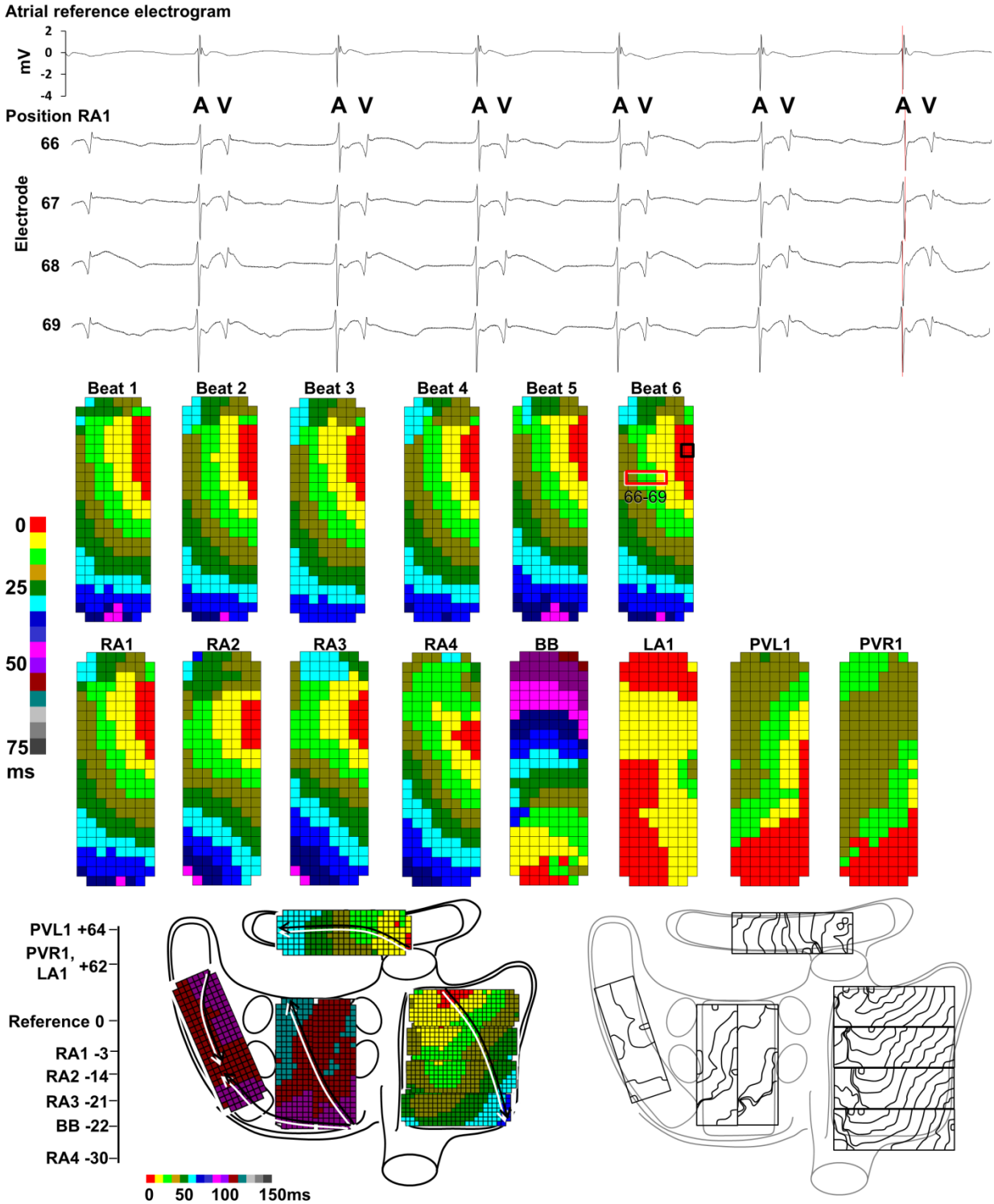

In the upper panel, the reference electrogram as well as the electrograms recorded at mapping position RA1 at electrode 66, 67, 68, and 69 are shown. In each electrogram, an atrial potential (A) and a farfield ventricular potential (V) can be distinguished. At position RA1, 6 successive SR beats were recorded. Activation maps were constructed by marking the steepest negative slope of the unipolar electrograms. In the last beat (no. 6), the steepest negative slopeof all unipolar electrograms is annotated by a red line. Activation maps of all beats recorded at RA1 are displayed. In beat number 6, electrodes 66-69 are marked by a red square. For each activation map, the earliest activated electrode, as annotated in the electrograms, is the marked as t=0. In the example of beat 6, the electrode marked by the black square is the earliest activated electrode, local activation times of electrodes 66, 67, 68 and 69 are respectively 15, 13, 11 and 8ms after the earliest activated electrode.

Similar to the construction of each activation map, the reference electrogram allows time alignment of the various recorded mapping positions, by correcting for the time intervals between activation maps. In this way, the total activation map, a view in which maps are thus time aligned, can be displayed. For further clarification of details of patterns of activation the corresponding isochronal maps are displayed next to the total SR map, in which isochrones are drawn at every 5ms.

A: atrial; BB: Bachmann's bundle; LA: left atrium; RA: right atrium; PVL: pulmonary veins left; PVR: pulmonary veins right; V: ventricular